UV Absorption Cross Sections, Laser Photodissociation Product Quantum Yields, and Reactions of H Atoms with Methylhydrazines at 298 K

Ghanshyam L. Vaghjiani

Hughes STX, Phillips Laboratory, PL/RKS, 10 E. Saturn Blvd, Edwards Air Force Base, California 93524

Received: December 10, 1996; In Final Form: March 31, 1997[⊗]

The gas-phase photochemistry of the diamines monomethylhydrazine (CH_3NHNH_2) and unsymmetrical dimethylhydrazine ($(CH_3)_2NNH_2$) has been studied in the ultraviolet (UV) at 298 K. Relative UV absorbance spectra of dilute mixtures of the diamine in He buffer gas were recorded in the region 140−310 nm with an instrument resolution of 0.25 nm. These were converted to absolute absorption cross section profiles by scaling the data with absolute 253.65-nm cross section values of $\sigma_{253.65} = (8.022 \pm 0.481) \times 10^{-20}$ and $(35.883 \pm 2.152) \times 10^{-20}$ cm^2 molecule^{-1} for CH_3NHNH_2 and $(CH_3)_2NNH_2$, respectively, which we also determined in this work. Both compounds exhibit continuous diffuse absorption bands in the UV that correspond to electronic transitions to dissociative singlet excited states. Laser photodissociation product measurements revealed the absolute H atom primary quantum yields to be $\Phi_{248} = 1.07 \pm 0.02$, $\Phi_{222} = 0.99 \pm 0.01$, and $\Phi_{193} = 0.94 \pm 0.07$ for CH_3NHNH_2 photolysis at 248, 222, and 193 nm, respectively. The corresponding values for $(CH_3)_2NNH_2$ photolysis were $\Phi_{248} = 0.97 \pm 0.06$, $\Phi_{222} = 0.91 \pm 0.06$, and $\Phi_{193} = 0.90 \pm 0.04$. Kinetic measurements gave the absolute second-order H atom rate coefficients to be $k = (7.60 \pm 1.14) \times 10^{-13}$ and $(13.48 \pm 2.02) \times 10^{-13}$ cm^3 molecule^{-1} s^{-1} respectively for reactions with CH_3NHNH_2 and $(CH_3)_2NNH_2$ at 298 K and in 26.0 Torr of He. Trends in the UV absorption cross section profiles, photodissociation product distributions, and the H atom reactivities in the homologous diamine series $(CH_3)_2NNH_2$, CH_3NHNH_2, and N_2H_4 are discussed.

Introduction

Unsymmetrical dimethylhydrazine ($(CH_3)_2NNH_2$), monomethylhydrazine (CH_3NHNH_2), and hydrazine (N_2H_4) are important rocket fuels. The combustion of these diamine propellants by nitrogen tetroxide (N_2O_4) in rocket motors provides propulsion for numerous systems such as for the Space Shuttle in low earth orbit and for the Titan vehicles during launch. Many of the elementary reactions that occur during propellant combustion are not well understood. Laboratory reaction kinetics studies on the decomposition mechanisms of the diamines are needed for carrying out propellant combustion modeling studies. We have chosen to quantify the concentration of the propellant vapor in our laboratory reactors by ultraviolet (UV) photometry. This "*in-situ*" method of determining the reactant concentration should be free from possible systematic errors associated with the handling of monometrically prepared diamine/He samples which are known to be susceptible to decomposition inside the gas flow lines.[1,2] The UV photometric method requires the use of accurate absolute UV absorption cross sections of the propellant vapors. Also, a knowledge of the UV absorption cross section profiles is important in quantifying electronic absorption oscillator strengths and the absolute photodissociation product distributions and in elucidating the nature of the excited states and potential energy surfaces involved during photolysis of the diamine molecules.

In the case of N_2H_4, numerous photochemical studies have been reported in the literature. We recently gave a brief review of these earlier reports and, where possible, made comparisons of our new UV absorption cross section values in the range 191−291 nm[1] to those in the literature. We also reported first direct measurements on the photodissociation product yields at 193, 222 and 248 nm.[1,3] For the alkylated diamines, photochemical data are sparse in the literature. Two recent studies have reported the UV absorption cross sections for $(CH_3)_2NNH_2$ and CH_3NHNH_2. Syage et al. measured the spectrum in the wavelength range from 115 to ∼240 nm,[4] while Lang carried out measurements in the range 115−185 nm.[5] The CH_3NHNH_2 spectra from these studies are only similar in shape and intensity in the region 145−185 nm and disagree considerably for wavelengths shorter than 145 nm. The $(CH_3)_2NNH_2$ spectra are similar neither in shape nor in intensity in the common region of study from 115 to 185 nm. For practical reaction kinetics studies, accurate near-UV absorption cross sections are desirable because of the ease in implementing a photometric absorption cell under atmospheric conditions and since numerous atomic line sources that operate in this wavelength range are readily available. Furthermore, since a small amount of water may ordinarily be present in the liquid diamine samples, any introduction of this into the reactor (during the gasification process of the sample) will not affect the photometric measurements as H_2O is essentially transparent to wavelengths longer than ∼190 nm. To our knowledge, no reliable near-UV absorption cross section data are available in the literature for the alkylated diamines. Also, only a limited number of end-product analysis studies have been carried out to elucidate what the primary products are in the photolysis of $(CH_3)_2NNH_2$[6] and its symmetrical isomer, $CH_3NHNHCH_3$.[7] From the distributions of the stable products observed, Overman and Wigg[6] concluded that the primary process was the fission of the relatively stronger N−H bond and not the weaker N−N bond in the 214.4-nm photolysis of unsymmetrical dimethylhydrazine. Kay and Taylor[7] reported the continuous UV absorption coefficients for symmetrical dimethylhydrazine in the range from 220 to ∼280 nm and studied its photolysis using several different light sources. No significant variation in the distribution of the stable products with wavelength was observed, and a mechanism that involved the breaking of the N−H bond was proposed to be the main process in the photolysis of this molecule also. No

[⊗] Abstract published in *Advance ACS Abstracts,* May 15, 1997.

S1089-5639(96)04044-3 CCC: $14.00

primary quantum yield data are to be found in the literature for CH_3NHNH_2 photolysis.

In an attempt to make comparisons to the existing vacuum-UV spectra and provide new data in the near-UV, we present here the absolute absorption cross sections in the range 140−310 nm for $(CH_3)_2NNH_2$ and CH_3NHNH_2 at 298 K. Our previous N_2H_4 absorption cross section data are now extended into the vacuum-UV. To further extend and quantify the primary H atom product yield measurements in diamine photolysis, we report here the room temperature laser photodissociation of CH_3NHNH_2 and $(CH_3)_2NNH_2$ at 193, 222, and 248 nm. First direct measurements of the absolute second-order rate coefficients for reactions of H atoms with these two diamine molecules were also determined.

Experimental Technique

Ultraviolet Absorption Spectra Measurements. The relative UV absorbance spectrum of a column of helium plus the alkylated diamine gas mixture which was slowly flowing across an absorption cell was determined in the region 140−310 nm at 298 K. The data in the wavelength range 210−310 nm was recorded at 600 Torr in a 49.8-cm-long Pyrex cell using the previously described diode-array spectrometer and D_2 lamp[1,8] while that in the range 140−220 nm at 8.0 Torr in a 10-cm-long Pyrex cell using a computer-controlled scanning vacuum monochromator equipped with a solar-blind photomultiplier tube (PMT).[9] The instrument resolution in both cases was typically 0.25 nm, full width at half-maximum (fwhm). The absorbance data were collected in 30−50-nm-wide segments. For a given segment the absorbance, $A = \ln[(I_0 - B)/(I_t - B)]$, was calculated as a function of wavelength, λ, where I_0 is the light signal recorded when only He flowed in the absorption cell and I_t that when the diamine was also present. B is the instrument background noise signal with the light source blocked off. The data in each segment were sufficiently averaged to improve the signal-to-noise ratio. The calculated absorbance data of a segment was checked to see that it obeyed the Beer−Lambert law (for absorbances of less than 1) by sufficiently varying the amount of diamine in the He carrier gas. The D_2 lamp and detector stability was better than 0.1% over the 15 min duration for recording a segment, and data with absorbances less than 0.002 were ignored. Adjacent segments were normalized to each other using the mean overlap factor observed at 0.25 nm intervals within the common region of 5−10 nm to facilitate the construction of the entire spectrum. The short and long wavelength limits of the continuous absorbance data we report here are determined by the lack of suitable intensity of the D_2 lamp below 140 nm and by the negligible absorption by the diamine beyond 310 nm even at saturated vapor conditions.

The absolute absorption spectra for CH_3NHNH_2 and $(CH_3)_2NNH_2$ vapors were obtained by scaling the above absorbance data with the absolute 253.65-nm cross section values, $\sigma_{253.65}$. These were calculated by applying the Beer−Lambert law to the observed attenuation of the 253.65-nm Hg line that occurred across the 49.8-cm-long absorption cell containing the alkylated diamine in a known excess of He flowing at 600 Torr and 298 K and quantifying the diamine vapor concentration by collecting the eluting diamine in a trap maintained at 77 K followed by iodometric titration of the condensate.[10] Upon establishing a stable flow of diamine/He as seen by the I_t signal being recorded, the flow exiting the absorption cell was diverted into the cold trap to collect the diamine. The collection efficiency of the trap is known to be >99%.[1] Excess He was slowly pumped off from the isolated trap, and the condensate warmed to 273 K, whereupon it was acidified with an excess of 4 M HCl acid under N_2 before letting it up to the atmosphere. The acidified mixture is stable to O_2 oxidation and can be titrated with standard 0.2 M KIO_3 solution with a few cubic centimeters of CCl_4 added to the aliquot to act as an indicator. Provided that the molarity of the solution is maintained above 3 M, quantitative oxidation of the diamine takes place according to the equations $CH_3NHNH_2 + KIO_3 + 2HCl \rightarrow N_2 + CH_3OH + KCl + ICl + 2H_2O$ and $2(CH_3)_2NNH_2 + KIO_3 + 2HCl \rightarrow (CH_3)_2NN{=}NN(CH_3)_2 + KCl + ICl + 3H_2O$. For the latter reaction it is important to maintain the aliqout between 268 and 278 K to prevent side reactions from occurring between KIO_3 and $(CH_3)_2NNH_2$.[10] The CH_3NHNH_2 gas-phase number density, c(molecule cm^{-3}) = n/v (or = $2n/v$ for $(CH_3)_2NNH_2$) in the absorption cell was calculated from the determined KIO_3 titre, n(molecule), and the total volume, v(cm^3), of gas mixture eluted during the experiment at 600 Torr and 298 K. Previously calibrated electronic mass flow meters, capacitance manometers, and chromel−alumel thermocouples were used to record the total He flow rate and the absorption cell pressure and temperature.

Laser Photodissociation Product Yield Measurements. The pulsed laser photolyses of diamines we report here were carried out in an excess of He buffer gas under optically thin conditions and low laser fluences in a small Pyrex reactor described previously.[1,3] A small flow of He was passed through a liquid sample of the diamine to carry the vapor into an absorption cell maintained at 298 K where its mole faction was determined by 213.9- or 253.65-nm photometric measurements. This flow was further diluted in a known excess of He just before sending the mixture into the Pyrex reactor maintained at 298 K. Typically, the [photolyte] range was in the order of $10^{13}-10^{15}$ molecules cm^{-3} in our experiments. Excimer laser photolysis of the mixture produced a low concentration of H atoms, typically in the range from 1×10^{10} to 1×10^{12} molecules cm^{-3}. The linear flow rate of the gas mixture (in the range 5−20 cm s^{-1}) and the repetition rate of the pulsed laser (in the range 1−10 Hz) were so chosen such that the mixture was subjected to only one laser flash (of 20 ns duration) as it slowly passed across the photolysis zone. The pseudo-first-order H atom temporal profile produced in the photolysis was monitored in "real time" by CW resonance fluorescence detection of H(^{2}S) at 121.6 nm using photon counting and multichannel scaling techniques. Up to 5000 temporal profiles for a given photolytic condition were coadded to improve the signal-to-noise ratio.

Materials. The He (>99.9997%) carrier gas from U.S. Bureau of Mines and O_2 (>99.99%) from Big Three Industries were used as received. Hydrocarbon-free N_2H_4 (Viking Grade) from Edwards AFB, $(CH_3)_2NNH_2$ (>99.3%), and CH_3NHNH_2 (>99.5%) from Olin Chemicals were subjected to several freeze−thaw purification cycles at a greaseless vacuum line, and the purified distillates were dried over BaO or CaH_2.

Results

Absolute Absorption Cross Sections. Figure 1 shows a plot of the average 253.65-nm absorbance monitored across the absorption cell versus the diamine propellant concentration determined in the titration experiments. These concentration values were within ~±5% to those predicted from the calculated vapor flow being carried by the He in our saturating bubbler. Values of $\sigma_{253.65} = (8.022 \pm 0.481) \times 10^{-20}$ and $(35.88 \pm 2.15) \times 10^{-20}$ cm^2 molecule^{-1} are determined respectively for CH_3NHNH_2 and $(CH_3)_2NNH_2$ at 298 K from the slopes of the plots and the known path length of 49.8 cm of our absorption cell. These values were used to normalize the relative UV absorbance

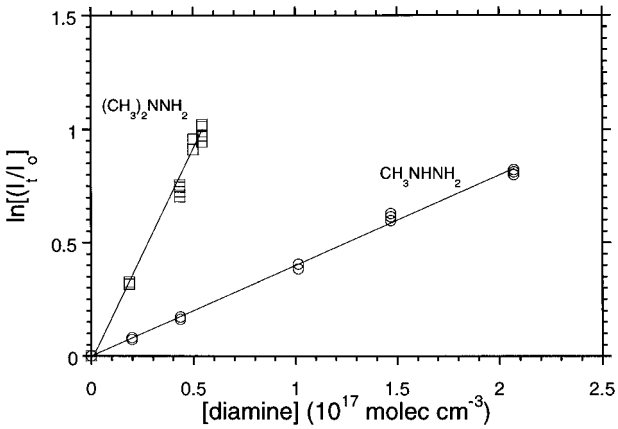

Figure 1. A plot of the gas-phase 253.65-nm absorbances measured at 298 K in the 49.8-cm-long absorption cell versus the concentration of the diamine propellant determined by titration with standard KIO_3 solution.

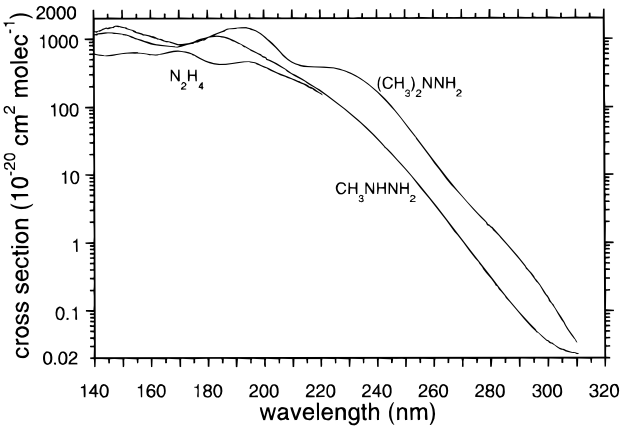

Figure 2. Gas-phase ultraviolet absorption cross section spectra of the diamines at 298 K.

TABLE 1: Ultraviolet Absorption Cross Sections of N_2H_4, CH_3NHNH_2, and $(CH_3)_2NNH_2$ Vapors at 298 K at a Selected Few Discrete Wavelengths[a]

wavelength (nm)	$\sigma_{N_2H_4}$	$\sigma_{CH_3NHNH_2}$	$\sigma_{(CH_3)_2NNH_2}$
121.6	1106.4	2506.3	2793.6
124.3	882.18	2149.9	2451.0
130.4	877.62	1866.7	2185.1
141.4	640.16	1153.0	1364.5
149.5	578.92	1189.6	1502.3
174.4	604.78	880.27	865.83

[a] The absorption cross sections, $\sigma_{diamine}$, are in the units of 10^{-20} cm^2 molecule^{-1}.

spectra to obtain the absolute cross section values in the range 140−310 nm for CH_3NHNH_2 and $(CH_3)_2NNH_2$. These cross section profiles are shown in Figure 2 which also includes new values for N_2H_4 which were normalized to our previous measurements.[1] For the interested reader, we provide Supporting Information tabulating the cross section data in 0.5-nm intervals.

By replacing the D_2 lamp with a He microwave discharge lamp, it was possible to determine relative UV absorbances at a selected few discrete wavelengths (121.6, 124.3, 130.4, 141.4, 149.5, and 174.4 nm) corresponding to characteristic strong atomic emission lines of the discharge. The 174.4-nm absorbance values were used to scale the above data set to absolute absorption cross sections using the 174.4-nm cross sections inferred from Figure 2. These are presented in Table 1, where the 141.6- and 149.5-nm data points of Table 1 are observed to be in very good agreement with those of Figure 2.

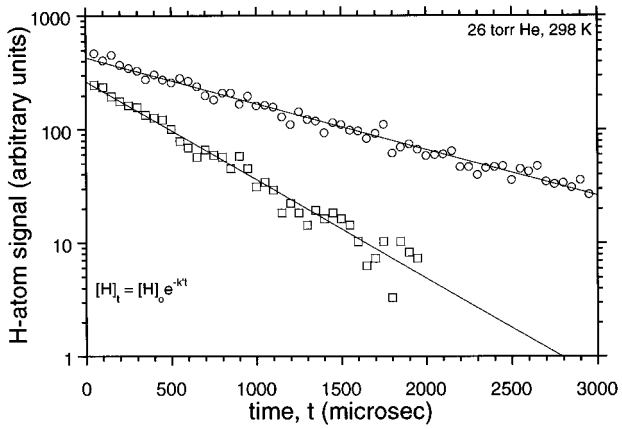

Figure 3. Typical H atom temporal profiles observed immediately after photolysis of the diamines, open circles is for $[CH_3NHNH_2] = 1.16 \times 10^{15}$ molecules cm^{-3} and open squares is for $[(CH_3)_2NNH_2] = 1.44 \times 10^{15}$ molecules cm^{-3}. The straight lines are exponential fits to the data points.

H Atom Quantum Yields and Reaction Rate Coefficients. Since the [diamine] is always in a great excess over the [H] produced in the photolysis, it can be shown that the temporal profile of H atoms immediately after photolysis is given by $[H]_t = [H]_0 e^{-k't}$, where $[H]_t$ and $[H]_0$ are the H atom concentrations at time t and zero, respectively. The constant k' ($= k$[diamine] $+ k_d$) is the pseudo-first-order rate coefficient for [H] decay in the photolyzed mixture. k_d is the sum of first-order rate coefficients due to, mainly, diffusion of H out of the detection zone and to, a small extent, reaction of H with background impurities. k is the absolute second-order rate coefficient for reaction of H atoms with the diamine. Figure 3 shows typical H atom temporal profiles obtained in CH_3NHNH_2 and $(CH_3)_2NNH_2$ photolyses. The data show instantaneous rises in the H atom signal upon photolyses and well-behaved exponential decays. The lines represent exponential fits to the data points. The slopes of the lines give values for the pseudo-first-order decay rate coefficients, k', and when the lines are extrapolated to time zero, the intercepts give a measure of the initial yields of H atoms in the photolyses.

The 248-nm laser photodissociation of $(CH_3)_2NNH_2$ (and CH_3NHNH_2) was studied relative to 248-nm photolysis of N_2H_4 in back-to-back runs at a constant laser fluence and where the microwave lamp probing the H atom formation is known to be stable over the course of the experiments. For the diamine under investigation, it can be shown that $\ln\{I_{0,diamine}/[diamine]\} = \ln\{I_{diamine}\} - K_{diamine}[diamine]$,[3,11] where $I_{0,diamine}$ is the observed initial H atom signal in the alkylated diamine photolysis and $K_{diamine}$ is proportional to the product of the effective path length and cross section for absorption of the fluorescence radiation in our experiments. For optically thin photolysis conditions, $I_{diamine}$ is directly proportional to the product $\Phi_{248}\sigma_{248}$, where Φ_{248} and σ_{248} are respectively the primary quantum yield for H atom production and absorption cross section for the alkylated diamine at 248 nm. Figure 4 shows typical data (open squares) obtained for 248-nm photolysis of $(CH_3)_2NNH_2$. The line is a fit to the data points using the above equation, and a value for $I_{diamine}$ is extracted from the intercept in the plot. Using the same analysis for N_2H_4 photolysis (open diamonds in Figure 4), it can be shown that $I_{diamine}/I_{N_2H_4} = (\Phi_{248}\sigma_{248})/(\Phi_{248,N_2H_4}\sigma_{248,N_2H_4})$. The values of Φ_{248,N_2H_4} equal to unity and $\sigma_{248,N_2H_4} = 5.88 \times 10^{-20}$ cm^2 molecule^{-1}, which we previously determined elsewhere,[1] were used to calculate $\Phi_{248} = 0.97 \pm 0.06$ for $(CH_3)_2NNH_2$ from the observed $I_{diamine}/I_{N_2H_4}$ ratio. A similar procedure for CH_3NHNH_2 photolysis at 248 nm gave $\Phi_{248} = 1.07 \pm 0.02$. The σ_{248} values for $(CH_3)_2NNH_2$ and CH_3-

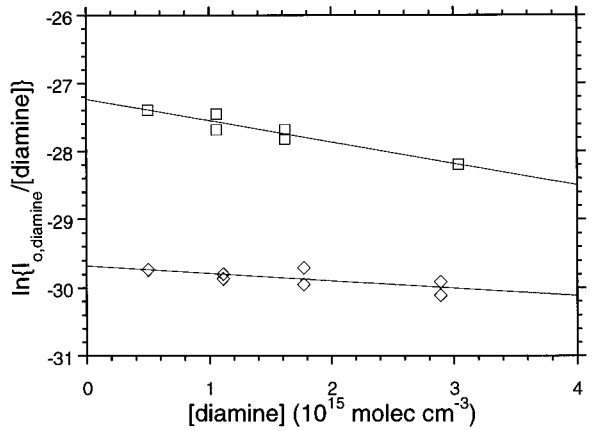

Figure 4. Plots showing the attenuation of the normalized initial H atom fluorescence signals (on a logarithmic scale) in N_2H_4 (open diamonds) and $(CH_3)_2NNH_2$ (open squares) photolyses at 248 nm and 298 K.

$NHNH_2$ were taken from Figure 2. The absolute second-order rate coefficients $k = (1.58 \pm 0.24) \times 10^{-13}$, $(7.60 \pm 1.14) \times 10^{-13}$, and $(13.48 \pm 2.02) \times 10^{-13}$ cm^3 molecule^{-1} s^{-1} for H atom reactions respectively with N_2H_4, CH_3NHNH_2, and $(CH_3)_2NNH_2$ were extracted from the slopes of plots of k' versus [diamine].

The 222-nm laser photodissociation of the alkylated diamine was studied relative to its photolysis at 248 nm. The outputs from two excimer lasers were carefully collimated and sent counterpropagating into the reactor to illuminate the same photolysis volume. Here, it can be shown that for a constant photolyte concentration the ratio $I_{0,222}/I_{0,248}$, of the initial H atom fluorescence signals in the two back-to-back experiments is given by $I_{0,222}/I_{0,248} = (\Phi_{222}/\Phi_{248})(\sigma_{222}/\sigma_{248})(N_{222}/N_{248})(E_{222}/E_{248})$, where Φ_{222} and Φ_{248} are the primary quantum yields, σ_{222} and σ_{248} the absorption cross sections, N_{222} and N_{248} the number of photons per unit energy, and E_{222} and E_{248} the laser beam energies measured at 222 and 248 nm, respectively. A value for $\Phi_{222} = 0.99 \pm 0.01$ was extracted from the measured slope in a plot of $I_{0,222}/I_{0,248}$ versus E_{222}/E_{248}. When the photolyte was replaced with $(CH_3)_2NNH_2$, $\Phi_{222} = 0.91 \pm 0.06$ was determined.

A similar set of experiments were performed for 193-nm photolysis relative to the 222-nm photolysis just described above. $\Phi_{193} = 0.90 \pm 0.04$ and 0.94 ± 0.07 were determined respectively for $(CH_3)_2NNH_2$ and CH_3NHNH_2 photolyses. The latter value is entirely consistent with $\Phi_{193} = 0.98 \pm 0.10$ that is observed when 193-nm photodissociation of CH_3NHNH_2 is studied relative to 193-nm photolysis of N_2H_4.

Since very high quantum yields are observed in the photolyses, a value of unity is taken at the reference laser wavelength when determining each of the above four primary quantum yield values. It was also verified in the experiments that the observed initial H atom signal varied linearly with the laser fluence range (0.2−4.0 mJ pulse^{-1} cm^{-2}) employed to ensure that two-photon dissociation processes were not occurring in our photolysis reactor.

Discussion

All three diamines show similar broad band absorption features in the region 140−310 nm. The absorption cross sections are observed to increase with increased methylation in the diamine molecule. Proper interpretations of the intensities and in band positions and how they change across the homologous series must await for reliable *ab initio* calculations to become available for the ground and the excited state structures and potential energy surfaces and for the properties of the transition moment(s) involved in the UV absorption process(es) for the alkylated diamines. Previously, Staemmler[12] has used one such type of a calculation to rationalize some of the observed features of the UV absorption spectrum of N_2H_4. The role of electronic structure and geometry on dissociation has recently been explored by Syage and co-workers using molecular orbital analysis on excited states of $N_2H_4^+$.[4] The data we report here were obtained at an instrumental resolution of 0.25 nm fwhm. Increasing the resolution to ∼0.025 nm did not have any discernible effect on the shape or the strength of the diffuse bands. The relative shape of our N_2H_4 vacuum-UV spectrum is in reasonable agreement with the recent data of Lang,[5] Syage et al.,[4] and Biehl and Stuhl[13] (and with other older data discussed in ref 1) though the absolute cross section values differ. Lang's values on average are ∼38% larger and Syage et al.'s ∼17% smaller than ours, while those of Biehl and Stuhl on average are ∼28% larger than our values. (However, their data for $\lambda >$ ∼200 nm are in good agreement with our near-UV values.[1]) Also, the reported N_2H_4 spectrum of Syage et al. shows characteristic residual NH_3 features, presumably due to diamine decomposition in their chamber, which we do not see in this work as we conditioned our cell walls to minimize decomposition as described elsewhere.[1] For CH_3NHNH_2, Syage et al. report a spectrum that is similar in shape to ours, but their σ values are ∼25% smaller than ours. Lang's CH_3NHNH_2 data fall in between those of Syage et al. and our study. The shape of our $(CH_3)_2NNH_2$ spectrum is similar to that of Syage et al., who report cross sections values that are on average ∼17% smaller than ours. Lang's spectrum for this molecule is consistent neither with the data of Syage and co-workers nor with ours. The reported "double hump" centered around ∼152 nm is not present in these two studies, and Lang's minimum at ∼147 nm is apparently shifted to longer λ by ∼7 nm. Lang's absolute values for σ are generally larger by up to ∼27%, though they dip below our numbers for ($143 > \lambda < 149$ nm) by up to ∼25% and again for $\lambda >$ 180 nm by up to ∼17%. Possible interference to the measured absorption from symmetrical dimethylhydrazine ($CH_3NHNHCH_3$) in Lang's sample of $(CH_3)_2NNH_2$ could well be responsible for the observed differences in the shape of the spectrum in this wavelength region.[5]

In the long wavelength tail of the near-UV absorption, comparisons are not possible since there are no previous cross section values for the two alkylated diamines studied here. Since the estimated error in the absolute values of our cross sections is ∼±6% and the error in the relative values (i.e., the shape of the spectrum) ∼±1% or so, as discussed previously,[1] we believe that the present work provides the most reliable data set for use in quantitative photometric measurements of diamine propellant concentrations in laboratory reactors for carrying out gas-phase reaction kinetics studies. It should be noted that the discrete $\sigma_{121.6}$ values we have determined for the three diamines in this work are consistent, to within ∼±15%, to that predicted from the slopes of the plots in Figure 4.

The continuous nature of the spectra is indicative of excitation to states that are repulsive and therefore should lead to dissociation. The present photodissociation data indicate that, within experimental errors (precision plus systematic), unit dissociation of the diamine molecule occurs in the absorption of an ultraviolet photon. Thus, as in N_2H_4,[1] the alkylated diamine molecular excitation process in the Franck−Condon region predominantly accesses an excited electronic hypersurface that is dissociative along the N−H stretching coordinate and not along the N−N coordinate. Using the analogy of the observed relative weakening of the N−H and the strengthening

of the N−N bonds in the ionized state of hydrazine compared to those in the neutral ground state, it is possible that these type of bond energy changes also take place in other lower electronic excited states and that the internal energy of the photoexcited species is exclusively channeled along the most exothermic reaction coordinate. The detailed reasons for this selectivity in bond breaking in diamines remain to be addressed theoretically. Our direct H atom yields are consistent with the previous end-product analysis works of Overman and Wiig[6] and Kay and Taylor,[7] who respectively studied the photolysis of $(CH_3)_2NNH_2$ and $CH_3NHNHCH_3$. In order to place precise upper limits for the H atom primary quantum yields in alkylated diamine photolysis, it is necessary to experimentally verify the primary yield of NH_2 or other radicals, if any. (Direct NH_2 formation in N_2H_4 photolysis has previously been suggested,[13−15] whose yield though not measured must be small since we have shown H atoms to be the principal product in the photolysis.[1]) Also, the determination of photofragment angular distributions and fragment translational energy disposal using time-of-flight methods would be very useful in obtaining details of the dynamics of the photodissociation which occurs over the excited electronic potential energy surface(s). It should be noted that, in contrast to photolysis, thermal decomposition of N_2H_4 primarily yields two NH_2 fragments due to fission of the N−N bond in the ground electronic state.[16−18] The experiments suggested above are currently in progress in our laboratory.

To our knowledge we are the first to report the absolute second-order rate coefficient for H atom reactions with CH_3NHNH_2 and $(CH_3)_2NNH_2$. The 298 K rate coefficients were independent of the initial H atom concentration range employed in this work, indicating that interference from secondary reactions of H atoms with photolysis or reaction products is unimportant in the present *k* determinations. As methylation increases along the diamine homologous series N_2H_4, CH_3NHNH_2, and $(CH_3)_2NNH_2$, the H atom rate coefficient is seen to increase systematically. The reaction of H atom with N_2H_4 is known to proceed via the abstraction of H to form H_2.[3,19] The observed trend here is consistent with either increased importance of abstraction reaction at the methyl moiety or enhanced ability to abstract the H from the N−H bond site. From our measured value for the reaction rate coefficient of H atoms with N_2H_4, we calculate the per N−H bond reactivity of $\sim 0.4 \times 10^{-13}$ cm^3 s^{-1} for H abstraction. Assuming no major role of steric effects in $(CH_3)_2NNH_2$ and that the same N−H reactivity prevails, the per CH_3 group reactivity is determined to be $\sim 6.3 \times 10^{-13}$ cm^3 s^{-1}. This would then predict (using the same above assumptions) a total CH_3NHNH_2 rate coefficient of $\sim 7.6 \times 10^{-13}$ cm^3 molecule^{-1} s^{-1}. This is exactly what we have measured experimentally! Similar reactivity trends have also been observed for the reactions of OH radicals and O atoms with the above three diamines.[20]

However, the good agreement between the observed rate coefficient and the above analysis might just be fortuitous, since there is some evidence in the literature that the N−H bond strength might be varying in the alkylated diamines.[21−24] We might then expect a change in the reaction rate from the N−H site as well as from the (preferred) C−H sites of the methyl moiety, where reactivity of the C−H bond might also vary depending on the degree of methylation at the N center along the diamine homologous series. Precise conclusions as to which of the two effects is more important cannot yet be drawn. Studies using ND- or CD_3-substituted diamine analogs where kinetic isotope effects are measured and product identities and absolute branching yields are determined as a function temperature should help clarify the situation.

Acknowledgment. This work was supported by the Air Force Office for Scientific Research under Contract F04611-93-C-0005.

Supporting Information Available: Tabulated absorption cross sections for $(CH_3)_2NNH_2$, CH_3NHNH_2, and N_2H_4 (3 pages). See ordering information on any current masthead page.

References and Notes

(1) Vaghjiani, G. L. *J. Chem. Phys.* **1993**, *98*, 2123.
(2) Hanratty, T. J.; Pattison, J. N.; Clegg, J. W. *Ind. Chem. Eng. Anal.* **1950**, *43*, 1113.
(3) Vaghjiani, G. L. *Int. J. Chem. Kinet.* **1995**, *27*, 777.
(4) Syage, J. A.; Cohen, R. B.; Steadman, J. *J. Chem. Phys.* **1992**, *97*, 6072. Syage, J. A. *ibid.* **1992**, *97*, 6085.
(5) Lang, V. I. *J. Quant. Spectrosc. Radiat. Transfer* **1994**, *52*, 45.
(6) Overman, J. D.; Wigg, E. O. *J. Am. Chem. Soc.* **1946**, *68*, 320.
(7) Kay, W. L.; Taylor, H. A. *J. Chem. Phys.* **1942**, *10*, 497.
(8) Vaghjiani, G. L. *J. Chem. Phys.* **1993**, *99*, 5936.
(9) Vaghjiani, G. L. *UV-Mechanisms: Laboratory Photochemical Decomposition and Reaction Kinetics Studies of Diamine Rocket Propellants*; Phillips Laboratory: Edwards AFB, CA, 1997.
(10) Malone, H. E.; Anderson, D. M. W. *Anal. Chim. Acta* **1969**, *48*, 87.
(11) Talukdar, R. K.; Vaghjiani, G. L.; Ravishankara, A. R. *J. Chem. Phys.* **1992**, *96*, 8194.
(12) Staemmler, V. *Acta Phys. Pol.* **1988**, *A74*, 331.
(13) Beihl, H.; Stuhl, F. *J. Photochem. Photobiol. A: Chem.* **1991**, *59*, 135.
(14) Lindberg, P.; Raybone, D.; Salthouse, J. A.; Watkinson, T. M.; Whitehead, J. C. *Mol. Phys.* **1987**, *62*, 1297.
(15) Vinogradov, I. P.; Firsov, V. V. *Opt. Spectrosc. USSR* **1982**, *53*, 26.
(16) Diesen, R. W. *J. Chem. Phys.* **1963**, *39*, 2121. Meyer, E.; Olschewski, H. A.; Troe, J.; Wagner, H. G. *Symp. (Int.) Combust. Proc.* **1969**, *12*, 345 and references therein.
(17) Filseth, S. V.; Danon, J.; Feldmann, D.; Campbell, J. D.; Welge, K. H. *Chem. Phys. Lett.* **1979**, *63*, 615.
(18) Hack, W.; Rathmann, K. *Z. Phys. Chem. (Munich)* **1992**, *176*, 151.
(19) Stief, L. J.; Payne, W. A. *J. Chem. Phys.* **1976**, *64*, 4892.
(20) Vaghjiani, G. L. *J. Chem. Phys.*, to be submitted.
(21) Foner, S. N.; Hudson, R. L. *J. Chem. Phys.* **1968**, *49*, 3724; **1970**, *53*, 4377.
(22) Melius, C. F. *BAC-MP4 Heats of Formation and Free Energies*; Sandia National Laboratory: Livermore, CA, 1993.
(23) Benson, S. W. *Thermochemical Kinetics*; Wiley: New York, 1976.
(24) Chase, Jr., M. W.; Davies, C. A.; Downey, Jr., J. R.; Frurip, D. J.; McDonald, R. A.; Syverud, A. N. *J. Phys. Chem. Ref. Data* **1985**, *14* (Suppl. 1).